

# Use of Neuroanatomical Pattern Classification to Identify Subjects in At-Risk Mental States of Psychosis and Predict Disease Transition

Nikolaos Koutsouleris, MD; Eva M. Meisenzahl, MD; Christos Davatzikos, PhD; Ronald Bottlender, MD; Thomas Frodl, MD; Johanna Scheuerecker, BA; Gisela Schmitt, MD; Thomas Zetzsche, MD; Petra Decker, BA; Maximilian Reiser, MD; Hans-Jürgen Möller, MD; Christian Gaser, PhD

**Context:** Identification of individuals at high risk of developing psychosis has relied on prodromal symptomatology. Recently, machine learning algorithms have been successfully used for magnetic resonance imaging-based diagnostic classification of neuropsychiatric patient populations.

**Objective:** To determine whether multivariate neuroanatomical pattern classification facilitates identification of individuals in different at-risk mental states (ARMS) of psychosis and enables the prediction of disease transition at the individual level.

**Design:** Multivariate neuroanatomical pattern classification was performed on the structural magnetic resonance imaging data of individuals in early or late ARMS vs healthy controls (HCs). The predictive power of the method was then evaluated by categorizing the baseline imaging data of individuals with transition to psychosis vs those without transition vs HCs after 4 years of clinical follow-up. Classification generalizability was estimated by cross-validation and by categorizing an independent cohort of 45 new HCs.

**Setting:** Departments of Psychiatry and Psychotherapy, Ludwig-Maximilians-University, Munich, Germany.

**Participants:** The first classification analysis included 20 early and 25 late at-risk individuals and 25 matched HCs. The second analysis consisted of 15 individuals with transition, 18 without transition, and 17 matched HCs.

**Main Outcome Measures:** Specificity, sensitivity, and accuracy of classification.

**Results:** The 3-group, cross-validated classification accuracies of the first analysis were 86% (HCs vs the rest), 91% (early at-risk individuals vs the rest), and 86% (late at-risk individuals vs the rest). The accuracies in the second analysis were 90% (HCs vs the rest), 88% (individuals with transition vs the rest), and 86% (individuals without transition vs the rest). Independent HCs were correctly classified in 96% (first analysis) and 93% (second analysis) of cases.

**Conclusions:** Different ARMSs and their clinical outcomes may be reliably identified on an individual basis by assessing patterns of whole-brain neuroanatomical abnormalities. These patterns may serve as valuable biomarkers for the clinician to guide early detection in the prodromal phase of psychosis.

*Arch Gen Psychiatry.* 2009;66(7):700-712

## Author Affiliations:

Departments of Psychiatry and Psychotherapy (Drs Koutsouleris, Meisenzahl, Bottlender, Frodl, Schmitt, Zetzsche, and Möller and Mss Scheuerecker and Decker) and Radiology (Dr Reiser), Ludwig-Maximilians-University, Munich, Germany; Section of Biomedical Image Analysis, Department of Radiology, University of Pennsylvania, Philadelphia (Dr Davatzikos); and Department of Psychiatry, Friedrich-Schiller-University, Jena, Germany (Dr Gaser).

**T**HE FIRST MANIFESTATION OF psychosis constitutes the most active disease phase, affecting the individual at both environmental and neurobiological dimensions.<sup>1</sup> Neurotoxic processes may underlie this disease phase and may drive clinical deterioration, leading ultimately to the disabling, chronic state of the disorder.<sup>2</sup> Therefore, the duration of untreated psychosis may have a critical effect on the long-term clinical outcome in terms of the responsiveness to medical treatment, frequency of hospitalizations, and social and cognitive functioning.<sup>3,4</sup> Thus, the clinical focus has increasingly shifted to the early recognition and treatment of individuals in an at-

risk mental state (ARMS) of psychosis to postpone or even prevent the onset of the disease.<sup>5-7</sup>

Early recognition relies on valid diagnostic markers that facilitate the detection of disease-related signals in heterogeneous, subclinical populations. In this regard, clinical studies of individuals with ARMS have identified patterns of subtle experiential and behavioral abnormalities consisting of affective and basic symptoms as well as attenuated psychotic symptoms, which are frequently paralleled by deteriorating social functioning.<sup>8-11</sup> Currently, the detection of individuals with ARMS and the determination of the risk of disease transition depends on this subclinical symptomatology.

However, the overlap between prodromal symptoms and psychopathological phenomena found in the general population<sup>12,13</sup> challenges the reliable delineation of the ARMS. Thus, the low predictive validity of single prodromal symptoms limits their use as diagnostic markers for the purpose of early recognition at the *individual* level.<sup>14</sup> Moreover, the accurate detection of subtle clinical abnormalities demands skilled personnel in highly specialized mental health services. Therefore, suitable biological markers may enhance the early recognition of emerging psychosis. In this context, recent neuroimaging studies showed structural alterations in a number of brain regions, suggesting that the prodromal state is associated with patterns of subtle gray matter (GM) abnormalities within the temporal and frontal cortices, the limbic system, and the cerebellum.<sup>15-21</sup>

The diagnostic utility of these alterations in the clinical treatment of single individuals with ARMS is limited because (1) the expression of structural abnormalities may strongly depend on the individual neurobiological vulnerability and (2) neuroanatomical parameters derived from group-level neuroimaging studies show a considerable between-group overlap.<sup>22</sup> These limitations may be surmounted by a methodological shift to multivariate machine learning techniques. In this context, support vector machines (SVMs)<sup>23</sup> emerged as a powerful tool in a wide range of biomedical applications because of their ability to learn the categorization of complex, high-dimensional training data and to generalize the learned classification rules to unseen data.<sup>24</sup> Recent studies demonstrated the utility of SVMs in the neuroanatomical classification of Alzheimer disease and schizophrenia.<sup>25-29</sup>

Because SVMs have not been applied to the magnetic resonance (MR) imaging-based diagnostic evaluation of individuals with ARMS, we investigated their ability to detect different ARMSs by performing a classification of healthy controls (HCs) vs individuals with ARMS grouped into "early" or "late" high-risk samples (ARMS-E or ARMS-L). This 2-stage conceptualization of the ARMS<sup>30,31</sup> has been supported by recent neurocognitive, neurophysiological, and structural brain findings.<sup>32-35</sup> Furthermore, the SVMs' performance in predicting disease transition was evaluated in an ARMS subgroup having clinical follow-up information. This sample was divided into individuals with and without disease transition (ARMS-T and ARMS-NT), who were categorized relative to each other and to HCs. The classifiers' performance was evaluated by means of 5-fold cross-validation and by classifying an independent sample of HCs. We expected the individuals with ARMS-L and ARMS-T to be classified with higher accuracy than those with ARMS-E and ARMS-NT.

## METHODS

### PARTICIPANTS

Forty-five individuals with ARMS (28 men and 17 women with a mean [SD] age of 25.1 [5.8] years) were recruited at our Early Detection and Intervention Centre for Mental Crises, Ludwig-Maximilians-University. Potential individuals with ARMS were referred to the center by primary health care services and were examined according to a standardized inclusion criteria checklist with operationalized definitions of different types of pro-

prodromal symptoms: basic symptoms taken from the Bonn Scale for Assessment of Prodromal Symptoms<sup>10</sup> and attenuated psychotic (APs) and brief limited intermittent psychotic symptoms (BLIPSs) as defined by the Personal Assessment and Crisis Evaluation (PACE) criteria.<sup>9</sup> The recruitment protocol has been detailed previously.<sup>15</sup> In summary, potential individuals with ARMS meeting defined sets of state and/or trait markers were included in the study. Inclusion based on global functioning and trait factors required a 30-point or greater reduction in the *DSM-IV* Global Assessment of Functioning Scale and (1) a familial history of psychotic disorders in the first-degree relatives or (2) a personal history of prenatal or perinatal complications. Inclusion based on psychopathological state markers required at least 1 positive item in the basic symptom, APS, or BLIPS categories of the inclusion criteria checklist following specific time and duration criteria (**Box**).<sup>15,32,37</sup>

The ARMS cohort was dichotomized according to a 2-stage conceptualization of the ARMS distinguishing between nonpsychotic ARMS-E, with an increased risk of psychosis, and psychotic ARMS-L, with an imminent risk of full-blown psychosis.<sup>30,31</sup> The ARMS-E sample consisted of individuals *without* APs and BLIPSs who had had at least 1 basic symptom (Box) several times within the past 3 months, appearing first at least 12 months before study inclusion, *and/or* who met a global functioning and trait criterion. Following the PACE criteria,<sup>9,38</sup> the ARMS-L sample comprised individuals with at least 1 APS within the past 3 months, appearing several times per week, *and/or* with at least 1 BLIPS, spontaneously resolving within 1 week. Basic symptoms *and/or* global functioning and trait markers were not exclusion criteria for this sample. In addition, prodromal symptomatology was rated by means of the Positive and Negative Syndrome Scale and Montgomery-Åsberg Depression Rating Scale.<sup>39,40</sup>

Individuals with ARMS were regularly followed up for 4 years to detect shifts toward a different ARMS or a transition to psychosis.<sup>41</sup> In individuals meeting the transition criteria, schizophrenia spectrum disorders were diagnosed according to the *International Statistical Classification of Diseases, 10th Revision* diagnostic research criteria at the time of transition and after 1 year. Exclusion criteria were assessed by obtaining the personal and familial history by means of a semistructured clinical interview and involved (1) disease transition; (2) a past or present diagnosis of schizophrenia spectrum and bipolar disorders, as well as delirium, dementia, amnesic or other cognitive disorders, mental retardation, and psychiatric disorders due to a somatic factor, following the *DSM-IV* criteria; (3) alcohol or drug abuse within 3 months before examination; (4) past or present inflammatory, traumatic, or epileptic diseases of the central nervous system; and (5) any previous treatment with antipsychotics.

For the first analysis (HC vs ARMS-E vs ARMS-L), we randomly selected a sample of 25 HCs (HC<sub>1</sub>) from a previously described group of 75 HCs<sup>15</sup> to create a balanced design regarding group sizes. The HC<sub>1</sub> group was matched groupwise for age, handedness, and years of education to the ARMS-E and ARMS-L samples. A second matched HC sample (HC<sub>2</sub>) was used for the second analysis (HC vs ARMS-T vs ARMS-NT) by randomly removing 8 subjects from HC<sub>1</sub>. Finally, 45 new HCs (HC<sub>new</sub> group) were recruited for the external validation of these classification analyses. Any HCs with a past or present personal or familial history of neuropsychiatric conditions were excluded from the study. All participants provided their written informed consent before study inclusion. The study was approved by the local research ethics committee.

### MR IMAGING DATA ACQUISITION

The MR images were obtained on a 1.5-T system (Magnetom Vision; Siemens, Erlangen, Germany). Imaging was performed with a T1-weighted 3-dimensional magnetization pre-

**ARMS-E: Individuals With ARMS Without APSs and/or BLIPs**

1. Individuals had  $\geq 1$  of the following basic symptoms appearing within 12 months before study inclusion and several times per week during the past 3 months:

- Thought interferences
- Thought perseveration
- Thought pressure
- Thought blockages
- Disturbances of receptive language, either heard or read
- Decreased ability to discriminate between ideas and perception, fantasy and true memories
- Unstable ideas of reference (subject-centrism)
- Derealization
- Visual perception disturbances
- Acoustic perception disturbances

and/or

2. Individuals showed a reduction in Global Assessment of Functioning Scale score (*DSM-IV*) of  $\geq 30$  points (within the past year) combined with  $\geq 1$  of the following trait markers:

- First-degree relative with a lifetime diagnosis of schizophrenia or a schizophrenia spectrum disorder
- Prenatal or perinatal complications

**ARMS-L: Individuals With ARMS With or Without Basic Symptoms,  
With or Without Global Functioning and Trait Markers**

1. Individuals had  $\geq 1$  of the following APSs within the past 3 months, appearing several times per week for a period of  $\geq 1$  week:

- Ideas of reference
- Odd beliefs or magical thinking
- Unusual perceptual experiences
- Odd thinking and speech
- Suspiciousness or paranoid ideation

and/or

2. Individuals had  $\geq 1$  BLIPS, defined as the appearance of 1 of the following psychotic symptoms for  $< 1$  week (interval between episodes  $\geq 1$  week), resolving spontaneously:

- Hallucinations
- Delusions
- Formal thought disorder
- Gross disorganized or catatonic behavior

Abbreviations: APSs, attenuated psychotic symptoms; ARMS, at-risk mental state; ARMS-E, early ARMS; ARMS-L, late ARMS; BLIPs, brief limited intermittent psychotic symptoms.

<sup>a</sup>Adapted from Häfner et al.<sup>36</sup>

pared rapid-acquisition gradient echo sequence (repetition time, 11.6 milliseconds; echo time, 4.9 milliseconds; field of view, 230 mm; matrix,  $512 \times 512$ ; 126 contiguous axial sections of 1.5-mm thickness; and voxel size,  $0.45 \times 0.45 \times 1.5$  mm).

## MR IMAGING DATA PREPROCESSING AND DIMENSIONALITY REDUCTION

After inspection for artifacts and gross abnormalities, the images were segmented into GM, white matter, and cerebrospinal fluid tissue maps in native space by means of the VBM5 toolbox (<http://dbm.neuro.uni-jena.de>), an extension of the SPM5 software package (Wellcome Department of Cognitive Neurology, London, England). Details of this segmentation protocol have been described previously.<sup>15</sup> The estimated tissue maps of each individual were combined into a single volume with the values of GM, white matter, and cerebrospinal fluid set to 150, 250, and 10, respectively. Then, an established high-dimensional normalization algorithm<sup>42,43</sup> registered these volumes to the single-subject brain template of Montreal Neurological Institute. This elastic warping algorithm compensates for the interindividual

anatomical variation by establishing point correspondences between cortical, subcortical, and ventricular structures, thus achieving a better alignment of corresponding anatomical regions than the standard SPM5 normalization. The anatomical information is encoded in the volumetric changes occurring during normalization and is applied to the registered tissue maps, allowing for a regional analysis of volumes in normalized space (RAVENS). Similar to the "modulation" step used in voxel-based morphometry,<sup>44</sup> RAVENS maps allow for local comparisons in standard space that are equivalent to volumetric comparisons of the original tissue maps in native space.<sup>45</sup> The individual GM-RAVENS maps were proportionally scaled to the global GM volume computed from the native tissue maps. The effects of age and sex were removed from the data by calculating the partial correlations between these variables and the images.

We applied principal component analysis (PCA) to the proportionally scaled, age- and sex-corrected GM-RAVENS maps by projecting the number of correlated voxels to a number of uncorrelated principal components (PCs).<sup>46,47</sup> The PCA reduces (1) the computational complexity of classification caused by the high dimensionality of MR imaging

data and (2) the generalization error of classification by optimizing the number of PCs for data projection, thus maximizing the degree of anatomical information while minimizing the impact of noise.<sup>47</sup> This filtering effect of PCA increases both sensitivity and specificity of multivariate pattern recognition techniques compared with gaussian smoothing, which improves sensitivity at the cost of anatomical specificity.

The optimal PC number for data projection was determined by the peak overall classification accuracy across the whole range of possible PC numbers as defined by the respective population size.<sup>47</sup> Peak cross-validated classification accuracies were observed at  $n_{PC}=21/n_{PC}=17$  in the first/second SVM analysis. In addition, the effect of PCA on classification performance was evaluated in the second SVM analysis by skipping the dimensionality reduction step before classification (eTable 1 and eTable 2, <http://www.archgenpsychiatry.com>). Before the class membership of the test subjects was predicted, the mapping parameters computed for the PCA projection of the training data were applied to the test data. The PCA was performed by means of the Dimensionality Reduction Toolbox.<sup>48</sup>

## SVM CLASSIFICATION

The SVMs are multivariate artificial learning algorithms applied recently to the MR imaging–based classification of neuropsychiatric patient populations.<sup>26–29,46,49</sup> They represent supervised machine learning procedures in that they (1) learn about group differences in a training data set categorized by some a priori knowledge and (2) apply the learned model to the classification of new data.<sup>23,50,51</sup>

From the perspective of statistical learning theory, MR images can be regarded as points in a high-dimensional space. In our case, the dimensionality of this space was determined by the optimal number of uncorrelated PCs obtained by PCA. The SVM analysis started with a nonlinear transformation from the low-dimensional space of the individuals' PC loadings to a high-dimensional feature space. Nonlinear kernel transformations may have important advantages over linear mappings because they can handle classification problems with nonlinear relations between class labels and data instances (**Figure 1** A). We used the radial basis functions kernel because it facilitates the adaptive modeling of the interface between the classes and thus significantly improves classification performance.<sup>52,53</sup> Intuitively, the kernel matrix can be regarded as a similarity measure, meaning that data instances sharing similar features form clusters within the feature space.

The SVMs implement the principle of structural risk minimization<sup>23,50,51</sup> to learn a classification rule that guarantees generalizability to unknown data instances, avoiding both model overfitting and underfitting. Structural risk minimization is achieved through *large margin* classification, which determines the optimal separating hyperplane (OSH) between the training classes by maximizing the distance between the nearest data instances of opposite classes (Figure 1B). These instances are the *support vectors* because they show the smallest distance to the OSH. Instances further away from the OSH do not contribute to the discrimination. Thus, the algorithm focuses on subtle between-group differences and not on gross, easily detectable anatomical features.

The OSH can be used to predict the class membership of new data instances. For each new instance, the classifier produces an output consisting of the predicted class membership and the decision value measuring the distance of the new instance to the OSH. These decision values were used for constructing multi-class classifiers in which the class label with the maximum absolute decision value across the 3 binary SVMs decided the class

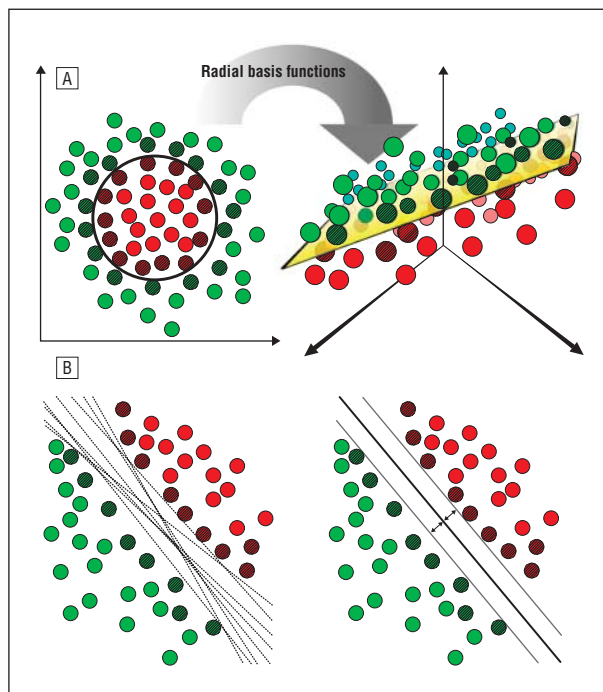


**Figure 1.** Schematic representation of nonlinear support vector machine (SVM) classification (A) and large-margin classification (B). A, At left, 2 groups of individuals (red and green shapes) cannot be separated in the input space by a linear classifier because the relationship between the data instances and their class labels is nonlinear (black circle). At right, With the use of radial basis functions, the data can be mapped into a high-dimensional space where the groups can be separated by means of linear classification. The shaded shapes represent the support vectors that define the optimal separating hyperplane (OSH) (yellow). B, At left, infinite separating boundaries (dotted lines) may exist between 2 classes (red and green circles). At right, the SVM algorithm determines the OSH by maximizing the margin between the nearest data instances of opposite classes.

membership (1-vs-1-by-maximum-wins method). We used the LIBSVM software for our SVM analysis.<sup>54</sup>

Although the SVM classifiers used in our analysis are effective in detecting spatially complex and subtle patterns of neuroanatomical between-group differences, they are difficult to visualize because of the nonlinearity of the classification method.<sup>53</sup> Discriminative neuroanatomical patterns were approximated by the following visualization technique: for all binary SVMs, the “nearest-neighbor” support vector pairs were determined by selecting support vectors from opposite classes that were separated by the smallest distance across the OSH. Then, the difference vector for each of these nearest-neighbor support vector pairs was calculated and the arithmetic mean of all difference vectors was formed. Finally, the PCs computed during the PCA procedure were weighted by the mean difference vector and summed to reconstruct the discriminative volume in the original space of the GM-RAVENS maps. For visualization purposes, the complexity of the discriminative patterns was reduced by smoothing the volumes with an isotropic gaussian kernel of 8 mm full width at half maximum. The patterns of the 3 binary classifiers were overlaid on the Montreal Neurological Institute single-subject anatomical template by means of the software package MRICron (<http://www.sph.sc.edu/comd/rorden/mricron/>).

## CLASSIFICATION PERFORMANCE

First, 5-fold cross-validation was performed to estimate the generalizability of the classification models.<sup>55</sup> Therefore, the study population was split into 5 nonoverlapping samples, and each



**Table 1. Statistical Analysis of Sociodemographic and Global Anatomical Parameters of Study Populations<sup>a</sup>**

Variable	HC <sub>1</sub>	HC <sub>2</sub>	HC <sub>new</sub>	ARMS-E	ARMS-L	<i>P</i> Value	ARMS-T	ARMS-NT	<i>P</i> Value
Sociodemographic variables									
No.	25	17	45	20	25		15	18	
Age at imaging, mean (SD), y	25.0 (5.5)	24.1 (4.8)	25.7 (4.1)	25.6 (5.7)	24.8 (6.0)	.86 <sup>b</sup>	25.9 (6.7)	22.4 (2.8)	.07 <sup>c</sup>
Sex, No. (%)						.28 <sup>d</sup>			.90 <sup>d</sup>
Male	19 (76)	11 (65)	29 (64)	10 (50)	18 (72)		11 (73)	11 (61)	
Female	6 (24)	6 (35)	16 (36)	10 (50)	7 (28)		4 (27)	7 (39)	
Handedness, No. (%) <sup>e</sup>						.63 <sup>d</sup>			.40 <sup>d</sup>
Right	21 (84)	14 (82)	40 (89)	17 (85)	22 (88)		15 (100)	14 (78)	
Left	3 (12)	2 (12)	5 (11)	2 (10)	1 (4)		0	3 (17)	
Ambidextrous	1 (4)	1 (6)	0	1 (5)	2 (8)		0	1 (6)	
Education, mean (SD), y	12.1 (1.3)	12.1 (1.4)	12.5 (0.9)	12.3 (0.9)	11.8 (1.4)	.07 <sup>b</sup>	12.3 (1.0)	11.8 (1.2)	.17 <sup>b</sup>
Global anatomical volumes, mean (SD), mm <sup>3</sup>									
GM	651.8 (88.7)	664.9 (95.9)	673.7 (56.7)	660.1 (62.7)	681.9 (78.4)	.42 <sup>b</sup>	653.7 (60.6)	698.0 (52.6)	.27 <sup>b</sup>
WM	523.9 (63.2)	530.2 (47.8)	543.4 (64.8)	527.7 (66.0)	531.0 (53.8)	.59 <sup>b</sup>	526.8 (63.0)	530.2 (47.8)	.53 <sup>b</sup>
CSF	456.8 (100.9)	446.5 (116.9)	470.1 (87.2)	446.5 (97.6)	475.2 (81.3)	.69 <sup>b</sup>	451.0 (97.6)	485.0 (97.8)	.62 <sup>b</sup>
VN	21.5 (9.3)	21.6 (9.7)	19.0 (9.0)	18.2 (6.2)	21.7 (10.0)	.40 <sup>b</sup>	18.9 (6.8)	28.1 (34.0)	.26 <sup>b</sup>
TI	1632.4 (215.6)	1630.2 (250.3)	1687.2 (163.4)	1634.2 (182.8)	1688.2 (156.4)	.47 <sup>b</sup>	1631.5 (177.8)	1713.1 (135.4)	.41 <sup>b</sup>

Abbreviations: ARMS, at-risk mental state; ARMS-E, early ARMS; ARMS-L, late ARMS; ARMS-NT, ARMS without disease transition; ARMS-T, ARMS with disease transition; CSF, cerebrospinal fluid; GM, gray matter; HC<sub>1</sub>, healthy control group 1; HC<sub>2</sub>, healthy control group 2; HC<sub>new</sub>, new healthy control group; TI, total intracranial; VN, ventricular; WM, white matter.

<sup>a</sup>Analyses of variance and *t* tests were performed for the sociodemographic and global anatomical variables either between HC<sub>1</sub>, HC<sub>new</sub>, ARMS-E, and ARMS-L samples or between HC<sub>2</sub>, HC<sub>new</sub>, ARMS-T, and ARMS-NT samples. *P* values of all tests are 2-sided.

<sup>b</sup>By 1-way analysis of variance.

<sup>c</sup>*P* = .03 in the post hoc analysis of ARMS-T vs ARMS-NT.

<sup>d</sup>By  $\chi^2$  test.

<sup>e</sup>Because of rounding, percentages may not total 100.

of these was iteratively held back as test data while the classifier was trained on the 4 remaining samples. In each iteration the class membership of the test data instances, which were unseen by the algorithm, was predicted by using the classifier constructed from the training data. Five-fold cross-validation provides a more conservative estimate of generalizability than leave-1-out cross-validation,<sup>56</sup> which iteratively predicts the class membership of only 1 test case against the rest of the population.<sup>28,56,57</sup> See also eTable 3 and eTable 4. Sensitivity, specificity, accuracy, false-positive rate, and positive (PPV) and negative predictive value (NPV) of cross-validation were computed for all binary and multiclass classifiers. Then, permutation testing was used to estimate the likelihood of obtaining classification performance *by chance*, meaning that the discriminative pattern between the data happened to correlate with the membership labels as an artifact of small sample sizes.<sup>58</sup> Therefore, the null distribution of the classification error was constructed for each classifier by performing 5000 random permutations of the membership labels and applying 5-fold cross-validation to each of these permutations. The null hypothesis that the classifier did not predict the test cases' class was rejected at  $\alpha = .05$ . Finally, the external validity of both multiclass classifiers was evaluated by predicting the class membership of HC<sub>new</sub>.

## RESULTS

**Table 1** and **Table 2** summarize the sociodemographic, clinical, and global anatomical characteristics of the study populations. No significant differences with respect to age, sex, handedness, years of education, and global brain volumes were found between the HC and ARMS samples except for age, which differed significantly between ARMS-T and ARMS-NT (Table 1). Reduced global functioning did not differ between ARMS-E and ARMS-L, but all 15 individuals

in the ARMS-T group showed a reduction of 30 points or more on the Global Assessment of Functioning Scale at study inclusion compared with 56% in the ARMS-NT sample (Table 2). The ARMS samples were not significantly different with respect to the prevalence of psychosis in the first-degree relatives or pre-natal and perinatal complications (Table 2).

No significant differences were detected between ARMS-E and ARMS-L regarding Positive and Negative Syndrome Scale and Montgomery-Åsberg Depression Rating Scale scores (Table 2). The ARMS-T group scored significantly higher on the Positive and Negative Syndrome Scale positive symptoms score and showed a trend toward a lower total Montgomery-Åsberg Depression Rating Scale score. The overall prevalence of cognitive basic symptoms (thought interference, thought perseveration, thought pressure, and thought blockages) was higher in the ARMS-L group than the ARMS-E group and in the ARMS-T group relative to the ARMS-NT group. The ARMS-T group showed a significantly higher prevalence of APSs and BLIPs than the ARMS-NT group at baseline (Table 2). In the ARMS-T sample, the mean time to transition was 188 days (range, 35-777 days). Thirteen individuals developed psychosis during the first year of follow-up, 1 person in the second year, and 1 person in the third year.

## NEUROANATOMICAL CLASSIFICATION

The permutation analysis showed that the classification models produced by all binary and multiclass SVM classifiers of our study were significant at  $P < .001$ . See also eTables 1 through 5.

**Table 2. Clinical Parameters and Outcome of ARMS Samples<sup>a</sup>**

Variables	ARMS	ARMS-E	ARMS-L	P Value	ARMS-T	ARMS-NT	P Value
<b>Clinical Variables</b>							
Global functioning and trait markers, No. (%) of subjects							
Family history of affective psychosis	5 (11.1)	3 (15.0)	2 (8.0)	.64 <sup>b</sup>	2 (13.3)	3 (16.7)	>.99 <sup>b</sup>
Family history of schizophrenic psychosis	6 (13.3)	2 (10.0)	4 (16.0)	.68 <sup>b</sup>	4 (26.7)	3 (16.7)	.67 <sup>b</sup>
GAF reduction >30%	32 (71.1)	13 (65.0)	19 (76.0)	.52 <sup>b</sup>	15 (100.0)	10 (55.6)	.004 <sup>b</sup>
Prenatal or perinatal complications	16 (35.6)	7 (35.0)	9 (36.0)	>.99 <sup>b</sup>	11 (73.3)	6 (33.3)	.30 <sup>b</sup>
Basic symptoms							
Individuals with >1 item, No. (%)	41 (91.1)	19 (95.0)	22 (88.0)	.62 <sup>b</sup>	13 (86.7)	16 (88.9)	.63 <sup>b</sup>
Item count, mean (SD)	3.0 (2.2)	2.4 (1.6)	3.5 (2.4)	.10 <sup>c</sup>	3.3 (2.2)	2.4 (1.9)	.20 <sup>c</sup>
Attenuated psychotic symptoms							
Individuals with >1 item, No. (%)	20 (44.4)	0	20 (80.0)	...	12 (80.0)	5 (27.8)	.005 <sup>b</sup>
Item count, mean (SD)	0.9 (1.2)	0.0 (0.0)	1.6 (1.2)	...	1.5 (1.0)	0.4 (0.7)	<.001 <sup>c</sup>
Brief limited intermittent psychotic symptoms							
Individuals with >1 item, No. (%)	17 (37.8)	0	17 (68.0)	...	8 (53.3)	4 (22.2)	.08 <sup>b</sup>
Item count, mean (SD)	1.0 (1.8)	0.0 (0.0)	1.8 (2.1)	...	1.3 (1.4)	0.3 (0.8)	.02 <sup>c</sup>
Other psychopathology scores, mean (SD)							
PANSS total score	54.4 (17.2)	50.2 (11.1)	56.6 (19.6)	.96 <sup>c</sup>	58.4 (22.1)	51.3 (11.2)	.11 <sup>c</sup>
PANSS positive score	10.8 (3.6)	9.3 (2.5)	11.7 (3.9)	.06 <sup>c</sup>	12.9 (4.5)	10.0 (2.4)	.03
PANSS negative score	14.3 (7.6)	12.9 (5.7)	15.1 (8.5)	.97 <sup>c</sup>	16.3 (9.0)	12.9 (5.6)	.06 <sup>c</sup>
PANSS general score	29.2 (8.2)	28.0 (5.8)	29.9 (9.3)	.48 <sup>c</sup>	29.3 (11.1)	28.5 (6.2)	.49 <sup>c</sup>
MADRS score	15.7 (8.5)	15.6 (8.8)	15.7 (8.6)	.27 <sup>c</sup>	11.1 (8.1)	17.1 (7.2)	.09 <sup>c</sup>
<b>Clinical Outcomes</b>							
Individuals with finished follow-up, No.	33	13	20				
Dropouts/unfinished follow-up, No.	12	7	5				
Individuals with ARMS-NT, No.	18	12	6				
Individuals with negative inclusion criteria	5	5	0				
Individuals meeting ARMS-E criteria	8	6	2				
Individuals meeting ARMS-L criteria	5	1	4				
Individuals with ARMS-T, No. (transition rate, %)	15 (45.5)	1 (7.7)	14 (70.0)				
Duration of transition, mean (range), d	188 (35-777)	777	142.6 (35-645)				
Diagnoses, No. of subjects							
Schizophrenia	10	1	9				
Schizoaffective disorder	4	0	4				
Schizotypal disorder	1	0	1				

Abbreviations: ARMS, at-risk mental state; ARMS-E, early ARMS; ARMS-L, late ARMS; ARMS-NT, ARMS without disease transition; ARMS-T, ARMS with disease transition; ellipses, not applicable; GAF, Global Assessment of Functioning Scale; PANSS, Positive and Negative Syndrome Scale; MADRS, Montgomery-Åsberg Depression Rating Scale.

<sup>a</sup>P values of all tests are 2-sided.

<sup>b</sup>By Fisher exact test.

<sup>c</sup>By *t* test.

### HC vs ARMS-E vs ARMS-L

The overall accuracy of the 3-group classifier was 81% (**Table 3**). Of 25 HC<sub>1</sub> individuals, 3 individuals were mislabeled as having ARMS-E and 2 as having ARMS-L (sensitivity, specificity, and accuracy for HC<sub>1</sub> vs the rest: 80%, 89%, and 86%, respectively). Two individuals with ARMS-E were mislabeled as having ARMS-L (ARMS-E vs the rest: 90%, 92%, and 91%, respectively). Of 25 individuals with ARMS-L, 5 were misclassified as being in the HC<sub>1</sub> group and 1 as having ARMS-E (ARMS-L vs the rest: 76%, 91%, and 86%, respectively). Among the binary classifiers, the highest accuracy of 87% (sensitivity, specificity, PPV, and NPV: 95%, 80%, 79%, and 95%, respectively) was observed for the classification of HC<sub>1</sub> vs ARMS-E, followed by 82% (84%, 80%, 84%, and 80%, respectively) for the ARMS-E vs ARMS-L classification and 78% (76%, 80%, 79%, and 77%, respectively) for the HC<sub>1</sub> vs ARMS-L classification (**Table 4**).

The discriminative pattern underlying the HC<sub>1</sub> vs ARMS-E classification consisted of GM volume reductions within the

cerebellum, thalamus, and prefrontal cortex bilaterally (**Figure 2A**). Further bilateral reductions were found in the medial occipital areas and precuneus, as well as in the lateral temporal lobe, including the middle and superior temporal gyrus and extending into the right supramarginal gyrus. Gray matter volume increments were detected within the inferior temporal lobes and lateral parietal cortices bilaterally. The HC<sub>1</sub> vs ARMS-L classifier relied on more extended and pronounced bilateral GM volume reductions in the cerebellum, precuneus, and supplementary motor areas, including the dorsomedial prefrontal cortex and anterior cingulate gyrus (**Figure 2B**). Further bilateral reductions were identified within the basal ganglia, orbitofrontal cortex, medial temporal lobes, and insula, as well as in the anterior portions of the superior temporal gyrus. The ARMS-E vs ARMS-L classification involved bilateral GM volume reductions occupying the anterior and posterior portions of the cingulate gyrus, the posterior part of the superior and middle temporal gyri with extensions into the inferior parietal lobule, the orbitofrontal and ventrolateral prefrontal cortex, and the cerebellum (**Figure 2C**).

**Table 3. Three-Group Classification Performance<sup>a</sup>**

HC vs ARMS-E vs ARMS-L				HC vs ARMS-T vs ARMS-NT			
Clinical Group	SVM Predicted Classes			Clinical Group	SVM Predicted Classes		
	HC <sub>1</sub>	ARMS-E	ARMS-L		HC <sub>2</sub>	ARMS-T	ARMS-NT
<b>Cross-validated SVM Performance</b>							
HC <sub>1</sub> , No.	20	3	2	HC <sub>2</sub> , No.	14	2	1
ARMS-E, No.	0	18	2	ARMS-T, No.	0	13	2
ARMS-L, No.	5	1	19	ARMS-NT, No.	2	2	14
Sensitivity, %	80	90	76	Sensitivity, %	82	87	78
Specificity, %	89	92	91	Specificity, %	94	89	91
Accuracy, %	86	91	86	Accuracy, %	90	88	86
FPR, %	11	8	9	FPR, %	6	11	9
PPV, %	80	82	83	PPV, %	88	77	82
NPV, %	89	96	87	NPV, %	91	94	88
Overall accuracy, %	81			Overall accuracy, %	82		
Model significance	<i>P</i> < .001			Model significance	<i>P</i> < .001		
<b>SVM Performance in Prediction of HC<sub>new</sub></b>							
HC <sub>new</sub> , No.	43	1	1	HC <sub>new</sub> , No.	42	3	0
Specificity, % <sup>b</sup>	96			Specificity, %	93		

Abbreviations: ARMS, at-risk mental state; ARMS-E, early ARMS; ARMS-L, late ARMS; ARMS-NT, ARMS without disease transition; ARMS-T, ARMS with disease transition; FPR, false-positive rate; HC, healthy control; HC<sub>1</sub>, HC group 1; HC<sub>2</sub>, HC group 2; HC<sub>new</sub>, new HC group; NPV, negative predictive value; PPV, positive predictive value; SVM, support vector machine.

<sup>a</sup>The multiclass SVM classifier was constructed by pairwise coupling of the binary SVM decision values obtained by 5-fold cross-validation. The class membership of an individual was determined by the classifier with the maximum decision value among all binary SVM classifiers. Classification performance was evaluated for 1 class against all other classes. The overall accuracy of the multiclass classifier was the proportion of all persons correctly classified by the algorithm. Sensitivity, specificity, accuracy, FPR, PPV, and NPV were calculated from the confusion matrix containing the number of true-positives, false-negatives, true-negatives, and false-positives. For example, 20 of 25 HC<sub>1</sub> subjects (sensitivity, 80%) were correctly assigned to their group, while 40 of 45 individuals with ARMS (89%) were correctly not labeled as HCs. Furthermore, the generalizability of classification was evaluated by classifying the independent HC<sub>new</sub> sample. The significance of multiclass classification was determined by 5000 random class label permutations.

<sup>b</sup>Measures the capability of a predictive model (in this case, HC vs ARMS-E vs ARMS-L and HC vs ARMS-T vs ARMS-NT) to identify the true-negatives in a population.

**Table 4. Two-Group Classification Performance<sup>a</sup>**

	Binary Classifiers					
	Analysis 1 <sup>b</sup>			Analysis 2 <sup>c</sup>		
	HC <sub>1</sub> vs ARMS-E	HC <sub>1</sub> vs ARMS-L	ARMS-E vs ARMS-L	HC <sub>2</sub> vs ARMS-T	HC <sub>2</sub> vs ARMS-NT	ARMS-T vs ARMS-NT
TP	19	19	21	15	14	15
TN	20	20	16	15	16	12
FP	5	5	4	2	1	3
FN	1	6	4	0	4	3
Sensitivity, %	95	76	84	100	78	83
Specificity, %	80	80	80	88	94	80
Accuracy, %	87	78	82	94	86	82
FPR, %	20	20	20	12	6	20
PPV, %	79	79	84	88	93	83
NPV, %	95	77	80	100	80	80
<i>P</i> value	<.001	<.001	<.001	<.001	<.001	<.001

Abbreviations: ARMS, at-risk mental state; ARMS-E, early ARMS; ARMS-L, late ARMS; ARMS-NT, ARMS without disease transition; ARMS-T, ARMS with disease transition; FN, false-negative; FP, false-positive; FPR, false-positive rate; HC, healthy control; HC<sub>1</sub>, HC group 1; HC<sub>2</sub>, HC group 2; NPV, negative predictive value; PPV, positive predictive value; TN, true-negative; TP, true-positive.

<sup>a</sup>The performance of the binary classification models was computed by means of 5-fold cross-validation. Sensitivity, specificity, accuracy, FPR, PPV, and NPV were calculated from the confusion matrix containing the number of TPs, FNs, TNs, and FPs. The significance of each binary classification was determined by 5000 random class label permutations.

<sup>b</sup>Neuroanatomical support vector machine analysis: 25 HCs vs 20 individuals with ARMS-E vs 25 individuals with ARMS-L.

<sup>c</sup>Neuroanatomical support vector machine analysis: 17 HCs vs 15 individuals with ARMS-T vs 18 individuals with ARMS-NT.

**HC vs ARMS-T vs ARMS-NT**

The overall accuracy of the 3-group classifier was 82%

(Table 3). Two of the 17 individuals in the HC<sub>2</sub> group were misclassified as having ARMS-T and 1 as having ARMS-NT (sensitivity, specificity, and accuracy for HC<sub>2</sub>

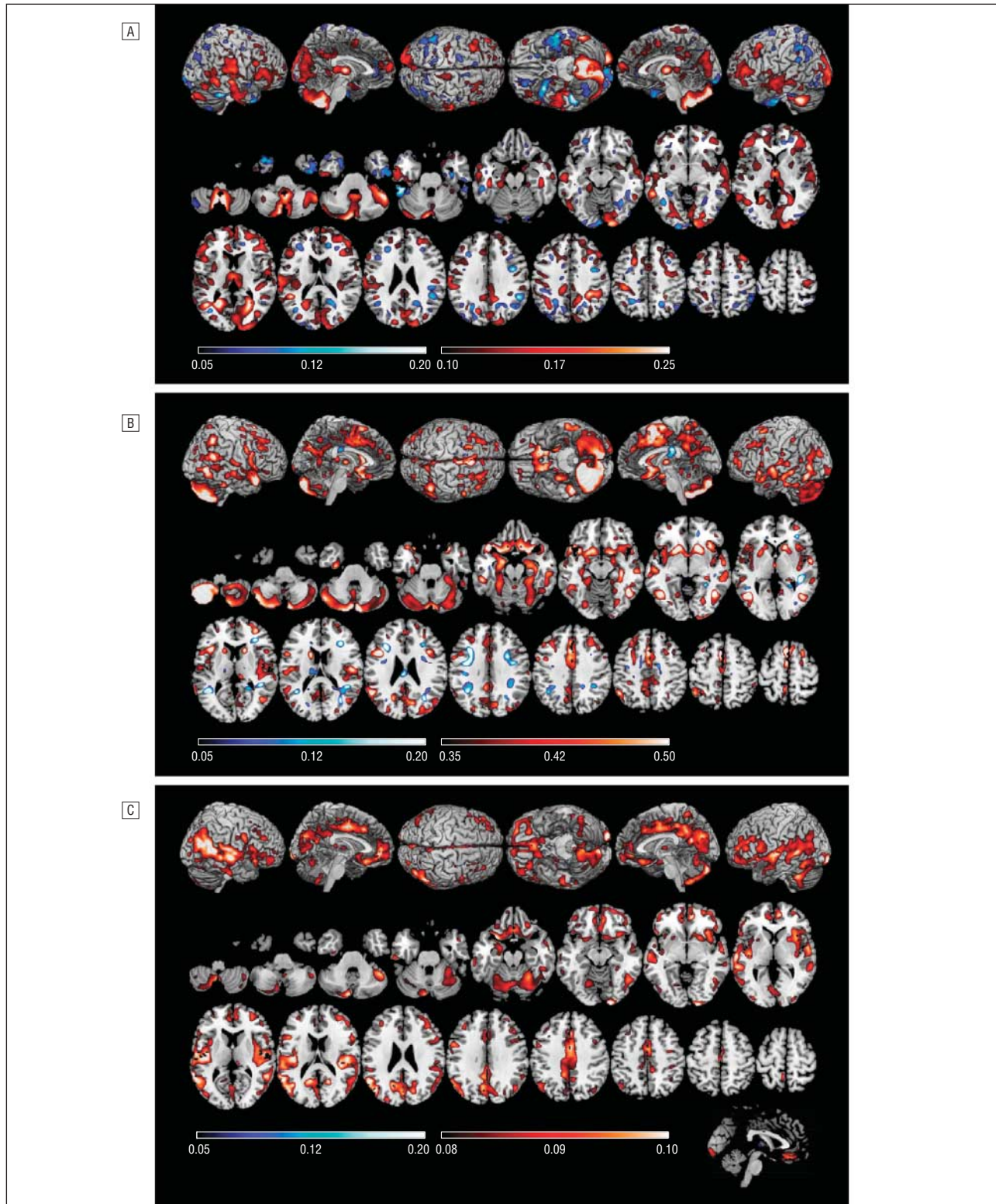


**Figure 2.** Discriminative patterns of the healthy control group 1 (HC<sub>1</sub>) vs at-risk mental state, early (ARMS-E) vs at-risk mental state, late (ARMS-L) classification analysis. See the “Methods” section for an explanation of the visualization technique. Warm and cool colors represent volumetric reductions and increments, respectively, in the second vs the first group of the binary classifier. The units are gray matter volume residuals (after removing the effects of age and sex by means of partial correlation analysis and after scaling to a range of [-1, 1]). The gray matter volume reduction scales differed between HC<sub>1</sub> vs ARMS-E (A), HC<sub>1</sub> vs ARMS-L (B), and ARMS-E vs ARMS-L (C), with the largest effects being observed in the HC<sub>1</sub> vs ARMS-L classifier and the most subtle differences being present in the discriminative pattern of ARMS-E vs ARMS-L.

vs the rest: 82%, 94%, and 90%, respectively). Two individuals with ARMS-T were wrongly assigned to the

ARMS-NT group (ARMS-T vs the rest: 87%, 89%, and 88%, respectively). Of the 18 individuals with ARMS-NT,



2 individuals were mislabeled as being in the HC<sub>2</sub> group and 2 as having ARMS-T (ARMS-NT vs the rest: 78%, 91%, and 86%, respectively). The binary classification of HC<sub>2</sub> vs ARMS-T attained the highest performance (accuracy, sensitivity, specificity, PPV, and NPV: 94%, 100%, 88%, 88%, and 100%, respectively), followed by the classification of HC<sub>2</sub> vs ARMS-NT (86%, 78%, 94%, 93%, and 80%, respectively) and ARMS-T vs ARMS-NT (82%, 83%, 80%, 83%, and 80%, respectively) (Table 4). In our additional analysis of the effect of dimensionality reduction on classification performance, we obtained significantly lower classification accuracies (HC<sub>2</sub> vs ARMS-T, 75%; HC<sub>2</sub> vs ARMS-NT, 51%; ARMS-T vs ARMS-NT, 70%; and 3-group classification, 60%) (eTables 1 and 2).

The HC<sub>2</sub> vs ARMS-NT and HC<sub>2</sub> vs ARMS-T classifications relied on similar GM volume reduction patterns occupying the anterior and posterior cingulate cortex; the orbitofrontal, lateral prefrontal, and inferior temporal cortex; and the medial temporal lobe and caudate nuclei bilaterally (Figure 3A and B). The discriminative pattern of HC<sub>2</sub> vs ARMS-T was more extended compared with HC<sub>2</sub> vs ARMS-NT. Finally, the ARMS-NT vs ARMS-T classifier detected a pattern of GM volume reductions involving the medial, lateral, and inferior temporal cortices, as well as the lateral prefrontal areas, the thalamus, and the cerebellum (Figure 3C).

#### COMMENT

To our knowledge, this is the first study to evaluate the feasibility of early recognition and disease prediction in individuals with ARMS by using multivariate neuroanatomical pattern classification. We were able to distinguish individuals with ARMS from HCs and to detect their ARMS with high diagnostic accuracy by relying solely on structural between-group differences. Furthermore, our study provided evidence that SVMs could be developed to predict transition to psychosis.

Our method's performance is comparable to that of previous neuroimaging studies that used SVMs for the diagnostic classification of Alzheimer disease, frontotemporal degeneration, and mild cognitive impairment.<sup>26,28,49</sup> Furthermore, MR imaging-based SVMs have been successfully applied to the categorization of schizophrenic patients<sup>29</sup> and their healthy relatives.<sup>27</sup> These studies demonstrate that MR imaging-based SVMs reliably separate different nosological populations at the individual level, suggesting good performance also in subclinical conditions.

#### BIOMARKERS OF ARMS-E AND ARMS-L

In our first SVM analysis (HC<sub>1</sub> vs ARMS-E vs ARMS-L), we observed a high cross-validated classification performance with the use of 2- and 3-group classifiers. The individuals with ARMS-L were recruited according to established ultrahigh-risk criteria (UHR), which were sensitive to an imminent risk of disease transition.<sup>7,8,38,41,59</sup> In this context, the cross-sectional and longitudinal clinical data of the ARMS-L sample (Table 1) were comparable to those of other UHR populations.<sup>7,8,38,41,59</sup> The high diagnostic accuracy of the

ARMS-L classifier suggests that structural patterns involving prefrontal, orbitofrontal, perisylvian, limbic, and cerebellar abnormalities may be associated with an imminent risk of full-blown psychosis in keeping with the results of previous investigations.<sup>15-19,21,60</sup> These studies showed that (1) UHR individuals show subtle structural brain abnormalities in similar brain regions as in patients with manifest schizophrenia and (2) subsequent conversion to psychosis may be associated with spatially more extended alterations at baseline and further progressive abnormalities during disease transition. Within this framework, our results suggest that neuroanatomical biomarkers of the UHR state could be integrated in future high-risk studies, as recently proposed.<sup>8</sup>

Contrary to our initial expectations, the individuals in the ARMS-E group were correctly assigned to their clinical group with an even higher accuracy, which may be owing to greater clinical heterogeneity of ARMS-L individuals caused by a significantly higher rate of disease transitions. Common psychopathological criteria are generally not sensitive to the early prodromal state because it largely overlaps with depressive syndromes<sup>61</sup> and nonspecific psychopathological phenomena found in the general population.<sup>12</sup> However, Klosterkötter et al<sup>10</sup> found a conversion rate of nearly 50% in 160 individuals with ARMS selected for an early prodromal state by the presence of perceptual-cognitive "basic symptoms."<sup>62</sup> In contrast, our ARMS-E conversion rate was 5.6%, although 10 highly predictive basic symptoms had been used as intake criteria (Box). This inconsistency may be due to our relatively small ARMS-E sample and the significantly shorter follow-up period. Recent findings suggest that different types of prodromes may exist, with 33% of the converters having prodromal phases lasting more than 6 years.<sup>63</sup>

Because of the low conversion rate of our ARMS-E sample, we do not know whether MR imaging-based SVMs would facilitate the prediction of a later disease transition in a putatively early prodromal stage of psychosis. Therefore, ARMS-E may rather be conceptualized as a *precursor* of psychosis<sup>64</sup> that is marked by increased disease vulnerability but that does not necessarily lead to a subsequent disease manifestation. Previous MR imaging studies of genetically defined at-risk individuals reported brain abnormalities in limbic and paralimbic structures<sup>17,18,21,65</sup> and in temporal and cerebellar regions.<sup>17</sup> Nonpsychotic subgroups within these populations may have similar abnormalities, albeit not to the extent found in individuals with ARMS-L.<sup>17,66</sup> The discriminative features used by the HC<sub>1</sub> vs ARMS-E classifier were consistent with these findings, but alterations of prefrontal, occipital, and thalamic structures may have additionally contributed to the good separability of ARMS-E. Our results suggest that subtle neuroanatomical abnormalities may underlie elevated disease vulnerability, potentially providing a valuable biomarker for the early precursors of psychosis.

#### PREDICTORS OF DISEASE TRANSITION

Our second analysis showed that SVMs are capable of distinguishing between ARMS-T and ARMS-NT individuals based on patterns of structural abnormalities present before the onset of psychosis. Lateral and medial tem-

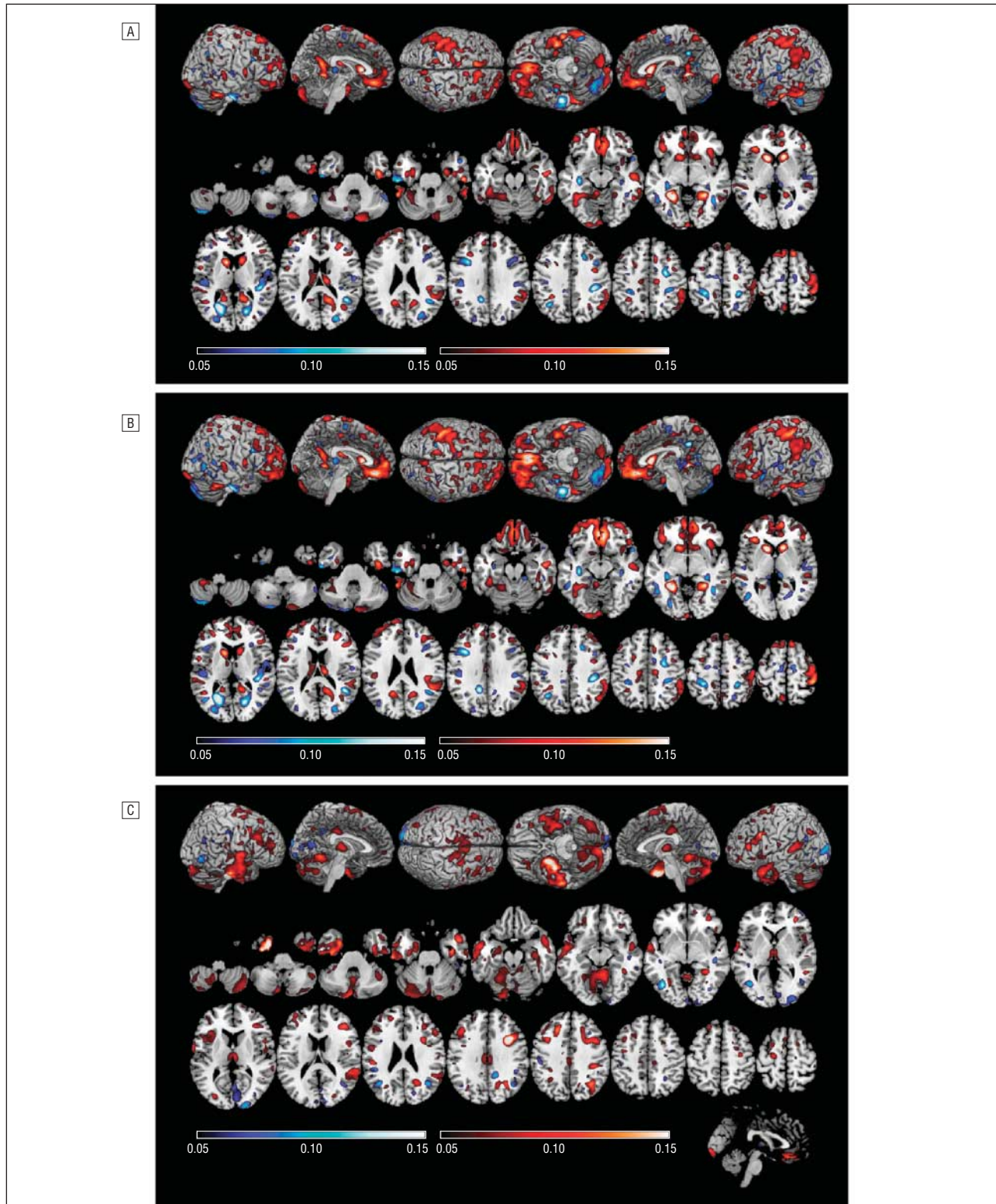


**Figure 3.** Discriminative patterns of the healthy control group 2 (HC<sub>2</sub>) vs at-risk mental state (ARMS) with disease transition (ARMS-T) vs ARMS without disease transition (ARMS-NT) classification analysis. A, HC<sub>2</sub> vs ARMS-T. B, HC<sub>2</sub> vs ARMS-NT. C, ARMS-T vs ARMS-NT. See the “Methods” section for an explanation of the visualization technique. Warm and cool colors represent volumetric reductions and increments, respectively, in the second vs the first group of the binary classifier.

poral abnormalities were found to separate converters from nonconverters, in keeping with previous voxel-based morphometric studies, which repeatedly showed that disease transition was associated with abnormalities of the perisylvian brain regions, the limbic and

paralimbic areas, and the anterior cingulate cortex at baseline<sup>19</sup> and over time.<sup>16,17,19,60</sup>

To date, only 1 study evaluated the feasibility of MR imaging-based psychosis prediction in a genetically defined ARMS population.<sup>67</sup> The authors found that lon-

itudinal GM density reductions in the inferior temporal gyrus predicted subsequent disease manifestation with a PPV of 60% and an NPV of 92%. These findings are not comparable to those of our study because the authors investigated *longitudinal* alterations in 3 regions of interest by using a univariate statistical procedure. Consistent with previous studies,<sup>26,28,29</sup> the high discriminative power of our classification method indicates that multivariate whole-brain techniques have significant advantages over region-of-interest methods because they capture the correlatedness of morphological features across the entire brain. Furthermore, our tool may be more suitable for clinical applications because follow-up images are not needed, thus allowing for a rapid assessment of at-risk individuals. This is crucial for early recognition because the current UHR criteria may be most sensitive to an imminent risk of disease transition.<sup>8</sup>

Our results suggest that neuroanatomical pattern recognition techniques may add further diagnostic reliability to multivariate algorithms<sup>8,9</sup> using clinical data for early recognition and disease prediction. In this regard, the high sensitivity observed in our classification analyses may compensate for the lower levels of sensitivity observed in the recently proposed clinical Cox regression models.<sup>8,9</sup> Furthermore, MR imaging-based diagnostic techniques may be more widely applicable because they (1) do not depend on highly specialized mental health services, (2) do not rely on unstable clinical measurements, and (3) potentially are not confined to ARMS populations that can be segregated by means of multivariate patterns of clinical data, meaning that these individuals are already considerably ill at clinical examination. Nevertheless, the operationalized psychopathological criteria underlying our ARMS-L definition facilitated the recruitment of a sample with 70% subsequent disease transitions.

The high accuracy of our classification technique was obtained by 5-fold cross-validation, which provides a conservative measure of generalizability because it iteratively tests an *independent* one-fifth of the population against the rest of the data. This is further supported by the reliable classification of HC<sub>new</sub> subjects. Both validation methods suggest that the early detection of individuals in different ARMSs of psychosis and the segregation of at-risk individuals who can expect a highly probable future disease manifestation could be achieved by SVM-based neurodiagnostic tools. However, this promising perspective does not imply that an individual admitted to the clinic with an ARMS-like pattern of psychopathological symptoms could be diagnosed with an equally high level of accuracy. This is because we used classifiers trained solely to categorize HCs and different ARMSs of psychosis as well as to predict a subsequent disease manifestation. It is unknown how strongly neuroanatomical "signatures" of other psychiatric disorders such as depression, bipolar disorder, or obsessive-compulsive disorder overlap with the discriminative patterns observed in different ARMSs of psychosis. Therefore, cross-nosological multigroup classifiers based on an SVM "library"<sup>28</sup> of different neuropsychiatric disorders and their prodromal stages may help to reliably differentiate the ARMS from other conditions.

Finally, further limitations have to be considered. First, an independent replication of our results is needed in larger ARMS populations. Second, our method may not be applicable as a general population screening procedure because we examined help-seeking individuals who overwhelmingly showed subclinical symptoms to a certain degree. Thus, it is unknown whether the method could distinguish completely asymptomatic, genetically defined high-risk individuals from HCs. Furthermore, it is unclear whether the method can be generalized across different MR imaging equipment. A recent study showed that SVMs reliably classified patients with Alzheimer disease even if training and test data were acquired from different imagers.<sup>28</sup> However, imager-induced noise will probably have a greater effect on the generalizability of the subtle neuroanatomical patterns underlying the ARMSs of psychosis.

In summary, our results suggest that SVM-based neuroanatomical pattern recognition techniques may substantially improve early-detection approaches that currently depend entirely on clinical information. Future projects may examine whether multimodal diagnostic tools integrating clinical, neuropsychological, neuroanatomical, and genetic markers could detect the ARMSs of psychosis and predict disease transition to a level of accuracy allowing for the preventive treatment of the disorder.

**Submitted for Publication:** July 22, 2008; final revision received November 12, 2008; accepted December 29, 2008.

**Correspondence:** Eva M. Meisenzahl, MD, Clinic of Psychiatry and Psychotherapy, Ludwig-Maximilians-University, Nussbaumstrasse 7, 80336 Munich, Germany (Eva.Meisenzahl@med.uni-muenchen.de).

**Author Contributions:** Drs Koutsouleris and Meisenzahl had full access to all the data in the study and take responsibility for the integrity of the data and the accuracy of data analysis. Drs Koutsouleris and Meisenzahl contributed equally.

**Financial Disclosure:** None reported.

**Funding/Support:** No funding was provided for the acquisition of MR imaging data. The Faculty of Medicine of the Ludwig-Maximilians-University (grant FöFoLe-444) provided financial support for the recruitment and clinical evaluation of the prodromal individuals. Furthermore, the development of methodological procedures used in this study was supported by the Federal Ministry for Education and Research research grants 01 EV0709 and 01 GW0740 (Dr Gaser).

**Role of the Sponsors:** The funding sources had no involvement in the study design, the collection and analysis of the data, or the writing of the manuscript.

**Additional Information:** The eTables are available at <http://www.archgenpsychiatry.com>.

**Additional Contributions:** Reinhold Bader, PhD (Linux Cluster Systems for the Munich and Bavarian Universities), integrated the VBM5 and HAMMER/RAVENS algorithms into the batch system of the Linux cluster. Fan Yong, MSc, and Xiaoying Wu, MSc (Section of Biomedical Imaging Analysis, University of Pennsylvania), provided excellent methodological support regarding the



implementation of the HAMMER/RAVENS algorithms, Chih-Jen Lin, PhD (National Taiwan University, Taiwan), helped adjust the LIBSVM software to the needs of neuroimaging analysis, and L. J. P. van der Maaten, MSc (Maastricht ICT Competence Centre, Universiteit Maastricht, Maastricht, the Netherlands), provided support regarding the use of the dimensionality reduction toolbox.

## REFERENCES

- McGlashan TH, Fenton WS. Subtype progression and pathophysiologic deterioration in early schizophrenia. *Schizophr Bull.* 1993;19(1):71-84.
- McGlashan TH, Zipursky RB, Perkins D, Addington J, Miller T, Woods SW, Hawkins KA, Hoffman RE, Preda A, Epstein I, Addington D, Lindborg S, Trzaskoma Q, Tohen M, Breier A. Randomized, double-blind trial of olanzapine versus placebo in patients prodromally symptomatic for psychosis. *Am J Psychiatry.* 2006;163(5):790-799.
- Perkins DO, Gu H, Boteva K, Lieberman JA. Relationship between duration of untreated psychosis and outcome in first-episode schizophrenia: a critical review and meta-analysis. *Am J Psychiatry.* 2005;162(10):1785-1804.
- Stephenson J. Delay in treating schizophrenia may narrow therapeutic window of opportunity. *JAMA.* 2000;283(16):2091-2092.
- Woods SW, Tully EM, Walsh BC, Hawkins KA, Callahan JL, Cohen SJ, Mathalon DH, Miller TJ, McGlashan TH. Aripiprazole in the treatment of the psychosis prodrome: an open-label pilot study. *Br J Psychiatry Suppl.* 2007;51:s96-s101.
- Phillips LJ, McGorry PD, Yuen HP, Ward J, Donovan K, Kelly D, Francey SM, Yung AR. Medium term follow-up of a randomized controlled trial of interventions for young people at ultra high risk of psychosis. *Schizophr Res.* 2007;96(1-3):25-33.
- Cornblatt BA. The New York high risk project to the Hillside recognition and prevention (RAP) program. *Am J Med Genet.* 2002;114(8):956-966.
- Cannon TD, Cadenhead K, Cornblatt B, Woods SW, Addington J, Walker E, Seidman LJ, Perkins D, Tsuang M, McGlashan T, Heinssen R. Prediction of psychosis in youth at high clinical risk: a multisite longitudinal study in North America. *Arch Gen Psychiatry.* 2008;65(1):28-37.
- Yung AR, Phillips LJ, Yuen HP, McGorry PD. Risk factors for psychosis in an ultra high-risk group: psychopathology and clinical features. *Schizophr Res.* 2004;67(2-3):131-142.
- Klosterkötter J, Hellmich M, Steinmeyer EM, Schultze-Lutter F. Diagnosing schizophrenia in the initial prodromal phase. *Arch Gen Psychiatry.* 2001;58(2):158-164.
- McGlashan TH. Early detection and intervention in schizophrenia: research. *Schizophr Bull.* 1996;22(2):327-345.
- Johns LC, Cannon M, Singleton N, Murray RM, Farrell M, Brugha T, Bebbington P, Jenkins R, Meltzer H. Prevalence and correlates of self-reported psychotic symptoms in the British population. *Br J Psychiatry.* 2004;185:298-305.
- Johns LC, Nazroo JY, Bebbington P, Kuipers E. Occurrence of hallucinatory experiences in a community sample and ethnic variations. *Br J Psychiatry.* 2002;180:174-178.
- Gottesman II, Erlenmeyer-Kimling L. Family and twin strategies as a head start in defining prodromes and endophenotypes for hypothetical early-interventions in schizophrenia. *Schizophr Res.* 2001;51(1):93-102.
- Meisenzahl EM, Koutsouleris N, Gaser C, Bottlender R, Schmitt GJE, McGuire P, Decker P, Burgermeister B, Born C, Reiser M, Möller HJ. Structural brain alterations in subjects at high-risk of psychosis: a voxel-based morphometric study. *Schizophr Res.* 2008;102(1-3):150-162.
- Borgwardt SJ, Riecher-Rössler A, Dazzan P, Chitnis X, Aston J, Drewe M, Gschwandtner U, Haller S, Pflüger M, Rechsteiner E, D'Souza M, Stieglitz RD, Radü EW, McGuire PK. Regional gray matter volume abnormalities in the at risk mental state. *Biol Psychiatry.* 2007;61(10):1148-1156.
- Job DE, Whalley HC, Johnstone EC, Lawrie SM. Grey matter changes over time in high risk subjects developing schizophrenia. *Neuroimage.* 2005;25(4):1023-1030.
- Job DE, Whalley HC, McConnell S, Glabus M, Johnstone EC, Lawrie SM. Voxel-based morphometry of grey matter densities in subjects at high risk of schizophrenia. *Schizophr Res.* 2003;64(1):1-13.
- Pantelis C, Velakoulis D, McGorry PD, Wood SJ, Suckling J, Phillips LJ, Yung AR, Bullmore ET, Brewer W, Soulsby B, Desmond P, McGuire PK. Neuroanatomical abnormalities before and after onset of psychosis: a cross-sectional and longitudinal MRI comparison. *Lancet.* 2003;361(9354):281-288.
- Lawrie SM, Whalley HC, Abukmeil SS, Kestelman JN, Donnelly L, Miller P, Best JJ, Owens DG, Johnstone EC. Brain structure, genetic liability, and psychotic symptoms in subjects at high risk of developing schizophrenia. *Biol Psychiatry.* 2001;49(10):811-823.
- Lawrie SM, Whalley H, Kestelman JN, Abukmeil SS, Byrne M, Hodges A, Rimmington JE, Best JJ, Owens DG, Johnstone EC. Magnetic resonance imaging of brain in people at high risk of developing schizophrenia. *Lancet.* 1999;353(9146):30-33.
- Davatzikos C. Why voxel-based morphometric analysis should be used with great caution when characterizing group differences. *Neuroimage.* 2004;23(1):17-20.
- Vapnik VN. An overview of statistical learning theory. *IEEE Trans Neural Netw.* 1999;10(5):988-999.
- Noble WS. What is a support vector machine? *Nat Biotechnol.* 2006;24(12):1565-1567.
- Fu CHY, Mourao-Miranda J, Costafreda SG, Khanna A, Marquand AF, Williams SCR, Brammer MJ. Pattern classification of sad facial processing: toward the development of neurobiological markers in depression. *Biol Psychiatry.* 2008;63(7):656-662.
- Fan Y, Batmanghelich N, Clark CM, Davatzikos C; Alzheimer's Disease Neuroimaging Initiative. Spatial patterns of brain atrophy in MCI patients, identified via high-dimensional pattern classification, predict subsequent cognitive decline. *Neuroimage.* 2008;39(4):1731-1743.
- Fan Y, Gur RE, Gur RC, Wu X, Shen D, Calkins ME, Davatzikos C. Unaffected family members and schizophrenia patients share brain structure patterns: a high-dimensional pattern classification study. *Biol Psychiatry.* 2008;63(1):118-124.
- Klöppel S, Stonnington CM, Chu C, Draganski B, Scahill RI, Rohrer JD, Fox NC, Jack CR Jr, Ashburner J, Frackowiak RSJ. Automatic classification of MR scans in Alzheimer's disease. *Brain.* 2008;131(pt 3):681-689.
- Davatzikos C, Shen D, Gur RC, Wu X, Liu D, Fan Y, Huggert P, Turetsky BI, Gur RE. Whole-brain morphometric study of schizophrenia revealing a spatially complex set of focal abnormalities. *Arch Gen Psychiatry.* 2005;62(11):1218-1227.
- Ruhrmann S, Schultze-Lutter F, Klosterkötter J. Early detection and intervention in the initial prodromal phase of schizophrenia. *Pharmacopsychiatry.* 2003;36(suppl 3):S162-S167.
- Salokangas RKR, McGlashan TH. Early detection and intervention of psychosis: a review. *Nord J Psychiatry.* 2008;62(2):92-105.
- Schultze-Lutter F, Ruhrmann S, Pickler H, von Reventlow HG, Daumann B, Brockhaus-Dumke A, Klosterkötter J, Pukrop R. Relationship between subjective and objective cognitive function in the early and late prodrome. *Br J Psychiatry Suppl.* 2007;51:s43-s51.
- Frommann I, Brinkmeyer J, Ruhrmann S, Hack E, Brockhaus-Dumke A, Bechold A, Wölwer W, Klosterkötter J, Maier W, Wagner M. Auditory P300 in individuals clinically at risk for psychosis. *Int J Psychophysiol.* 2008;70(3):192-205.
- Quednow BB, Frommann I, Berning J, Kühn KU, Maier W, Wagner M. Impaired sensorimotor gating of the acoustic startle response in the prodrome of schizophrenia. *Biol Psychiatry.* 2008;64(9):766-773.
- Hurlemann R, Jessen F, Wagner M, Frommann I, Ruhrmann S, Brockhaus A, Pickler H, Scheef L, Block W, Schild HH, Möller-Hartmann W, Krug B, Falkai P, Klosterkötter J, Maier W. Interrelated neuropsychological and anatomical evidence of hippocampal pathology in the at-risk mental state. *Psychol Med.* 2008;38(6):843-851.
- Häfner H, Maurer K, Ruhrmann S, Bechold A, Klosterkötter J, Wagner M, Maier W, Bottlender R, Möller HJ, Gaebel W, Wölwer W. Early detection and secondary prevention of psychosis: facts and visions. *Eur Arch Psychiatry Clin Neurosci.* 2004;254(2):117-128.
- Pukrop R, Ruhrmann S, Schultze-Lutter F, Bechold A, Brockhaus-Dumke A, Klosterkötter J. Neurocognitive indicators for a conversion to psychosis: comparison of patients in a potentially initial prodromal state who did or did not convert to a psychosis. *Schizophr Res.* 2007;92(1-3):116-125.
- Yung AR, Phillips LJ, Yuen HP, Francey SM, McFarlane CA, Hallgren M, McGorry PD. Psychosis prediction: 12-month follow up of a high-risk ("prodromal") group. *Schizophr Res.* 2003;60(1):21-32.
- Kay SR, Fiszbein A, Opler LA. The Positive and Negative Syndrome Scale (PANSS) for schizophrenia. *Schizophr Bull.* 1987;13(2):261-276.
- Montgomery SA, Åsberg M. A new depression scale designed to be sensitive to change. *Br J Psychiatry.* 1979;134:382-389.
- Yung AR, Phillips LJ, McGorry PD, McFarlane CA, Francey S, Harrigan S, Patton GC, Jackson HJ. Prediction of psychosis: a step towards indicated prevention of schizophrenia. *Br J Psychiatry Suppl.* 1998;172(33):14-20.
- Shen D, Davatzikos C. HAMMER: hierarchical attribute matching mechanism for elastic registration. *IEEE Trans Med Imaging.* 2002;21(11):1421-1439.
- Shen D, Davatzikos C. Very high-resolution morphometry using mass-preserving deformations and HAMMER elastic registration. *Neuroimage.* 2003;18(1):28-41.



44. Ashburner J, Friston KJ. Voxel-based morphometry: the methods. *Neuroimage*. 2000;11(6 pt 1):805-821.
45. Davatzikos C, Genc A, Xu D, Resnick SM. Voxel-based morphometry using the RAVENS maps: methods and validation using simulated longitudinal atrophy. *Neuroimage*. 2001;14(6):1361-1369.
46. Mourão-Miranda J, Bokde ALW, Born C, Hampel H, Stetter M. Classifying brain states and determining the discriminating activation patterns: support vector machine on functional MRI data. *Neuroimage*. 2005;28(4):980-995.
47. Hansen LK, Larsen J, Nielsen FA, Strother SC, Rostrup E, Savoy R, Lange N, Sidtis J, Svarer C, Paulson OB. Generalizable patterns in neuroimaging: how many principal components? *Neuroimage*. 1999;9(5):534-544.
48. van der Maaten L. *An Introduction to Dimensionality Reduction Using MatLab: Technical Report MICCIKAT 07-07*. Maastricht, the Netherlands: Maastricht University; 2007.
49. Davatzikos C, Fan Y, Wu X, Shen D, Resnick SM. Detection of prodromal Alzheimer's disease via pattern classification of magnetic resonance imaging. *Neurobiol Aging*. 2008;29(4):514-523.
50. Burges CJC. A tutorial on support vector machines for pattern recognition. *Data Mining Knowledge Discovery*. 1998;2:121-167.
51. Vapnik V. *Statistical Learning Theory*. New York, NY: Wiley Interscience; 1998.
52. Fan Y, Rao H, Giannetta J, Hurt H, Wang J, Davatzikos C, Shen D. Diagnosis of brain abnormality using both structural and functional MR images. *Conf Proc IEEE Eng Med Biol Soc*. 2006;1:1044-1047.
53. Lao Z, Shen D, Xue Z, Karacali B, Resnick SM, Davatzikos C. Morphological classification of brains via high-dimensional shape transformations and machine learning methods. *Neuroimage*. 2004;21(1):46-57.
54. Chang CC, Lin CJ. LIBSVM: a library for support vector machines, 2001. <http://www.csie.ntu.edu.tw/~cjlin/libsvm>. Accessed April 1, 2009.
55. Zhang P. Model selection via multi-fold cross validation. *Ann Stat*. 1993;21:299-313.
56. Kawasaki Y, Suzuki M, Kherif F, Takahashi T, Zhou SY, Nakamura K, Matsui M, Sumiyoshi T, Seto H, Kurachi M. Multivariate voxel-based morphometry successfully differentiates schizophrenia patients from healthy controls. *Neuroimage*. 2007;34(1):235-242.
57. Calder AJ, Burton AM, Miller P, Young AW, Akamatsu S. A principal component analysis of facial expressions. *Vision Res*. 2001;41(9):1179-1208.
58. Golland P, Fischl B. Permutation tests for classification: towards statistical significance in image-based studies. *Inf Process Med Imaging*. 2003;18:330-341.
59. Miller TJ, McGlashan TH, Rosen JL, Somjee L, Markovich PJ, Stein K, Woods SW. Prospective diagnosis of the initial prodrome for schizophrenia based on the Structured Interview for Prodromal Syndromes: preliminary evidence of interrater reliability and predictive validity. *Am J Psychiatry*. 2002;159(5):863-865.
60. Borgwardt SJ, McGuire PK, Aston J, Berger G, Dazzan P, Gschwandtner U, Pflüger M, D'Souza M, Radue EW, Riecher-Rössler A. Structural brain abnormalities in individuals with an at-risk mental state who later develop psychosis. *Br J Psychiatry Suppl*. 2007;51:s69-s75.
61. Klosterkötter J, Schultze-Lutter F, Gross G, Huber G, Steinmeyer EM. Early self-experienced neuropsychological deficits and subsequent schizophrenic diseases: an 8-year average follow-up prospective study. *Acta Psychiatr Scand*. 1997;95(5):396-404.
62. Gross G. The "basic" symptoms of schizophrenia. *Br J Psychiatry Suppl*. 1989;7(7):21-25, discussion 37-40.
63. Schultze-Lutter F, Ruhrmann S, Pickler H, von Reventlow HG, Brockhaus-Dumke A, Klosterkötter J. Basic symptoms in early psychotic and depressive disorders. *Br J Psychiatry Suppl*. 2007;51:s31-s37.
64. Maier W, Cornblatt BA, Merikangas KR. Transition to schizophrenia and related disorders: toward a taxonomy of risk. *Schizophr Bull*. 2003;29(4):693-701.
65. Keshavan MS, Dick E, Mankowski I, Harenski K, Montrose DM, Diwadkar V, DeBellis M. Decreased left amygdala and hippocampal volumes in young offspring at risk for schizophrenia. *Schizophr Res*. 2002;58(2-3):173-183.
66. Spencer MD, Moorhead TWJ, McIntosh AM, Stanfield AC, Muir WJ, Hoare P, Owens DGC, Lawrie SM, Johnstone EC. Grey matter correlates of early psychotic symptoms in adolescents at enhanced risk of psychosis: a voxel-based study. *Neuroimage*. 2007;35(3):1181-1191.
67. Job DE, Whalley HC, McIntosh AM, Owens DGC, Johnstone EC, Lawrie SM. Grey matter changes can improve the prediction of schizophrenia in subjects at high risk. *BMC Med*. 2006;4:29.

### Correction

**Error in Results.** In the Original Article by Barker et al titled "Developmental Trajectories of Male Physical Violence and Theft: Relations to Neurocognitive Performance," published in the May 2007 issue of the *Archives* (2007;64[5]:592-599), a computation error affected the conclusions drawn about the relationship between neurocognition and theft. The original conclusion stated in the "Results" section of the Abstract was that "Executive function and verbal IQ performance were negatively related to high frequency of physical violence but positively related to high frequency of theft." The sentence should have read "Executive function and verbal IQ performance were negatively related to high frequency of physical violence but were unrelated to theft."